Development 123, 67-80
Printed in Great Britain © The Company of Biologists Limited 1996
DEV3335

Mutations affecting cell fates and cellular rearrangements during gastrulation in zebrafish

Lilianna Solnica-Krezel[†], Derek L. Stemple, Eliza Mountcastle-Shah, Zehava Rangini[‡], Stephan C. F. Neuhauss, Jarema Malicki, Alexander F. Schier[§], Didier Y. R. Stainier[¶], Fried Zwartkruis, Salim Abdelilah and Wolfgang Driever***

Cardiovascular Research Center, Massachusetts General Hospital and Harvard Medical School, 13th Street, Bldg. 149, Charlestown, MA 02129, USA

[†]Present address: Department of Molecular Biology, Vanderbilt University, Box 1820, Station B, Nashville, TN 37235, USA
[‡]Present address: Department of Oncology, Sharett Institute, Hadassah Hospital, Jerusalem 91120, Israel
[§]Present address: Skirball Institute of Biomolecular Medicine, NYU Medical Center, 550 First Avenue, New York, NY 10016, USA
[¶]Present address: School of Medicine, Department of Biochemistry and Biophysics, UCSF, San Francisco, CA 94143-0554, USA
**Present address: Laboratory for Physiological Chemistry, Utrecht University, Universiteitsweg 100, 3584 CG Utrecht, The Netherlands
*Author for correspondence (e-mail: driever@helix.mgh.harvard.edu)

SUMMARY

One of the major challenges of developmental biology is understanding the inductive and morphogenetic processes that shape the vertebrate embryo. In a large-scale genetic screen for zygotic effect, embryonic lethal mutations in zebrafish we have identified 25 mutations that affect specification of cell fates and/or cellular rearrangements during gastrulation. These mutations define at least 14 complementation groups, four of which correspond to previously identified genes. Phenotypic analysis of the ten novel loci revealed three groups of mutations causing distinct effects on cell fates in the gastrula. One group comprises mutations that lead to deficiencies in dorsal mesodermal fates and affect central nervous system patterning. Mutations from the second group affect formation of ventroposterior embryonic structures. We suggest that mutations in these two groups identify genes necessary for the formation, maintenance or function of the dorsal organizer and the ventral signaling pathway, respectively. Mutations in the third group affect primarily cellular rearrangements during gastrulation and have complex effects on cell fates in the embryo. This group, and to some extent mutations from the first two groups, affect the major morphogenetic processes, epiboly, convergence and extension, and tail morphogenesis. These mutations provide an approach to understanding the genetic control of gastrulation in vertebrates.

Key words: organizer, gastrulation, epiboly, convergence, extension, zebrafish, dorsoventral polarity

INTRODUCTION

The vertebrate body plan is established by a series of inductive interactions and cellular rearrangements. Mechanisms underlying these processes are best understood in amphibia (Sive, 1993; Kessler and Melton, 1994; Slack, 1994). Vegetal blastomeres of the amphibian blastula are a source of signals that induce and pattern mesoderm in the overlying equatorial region (Nieuwkoop, 1969). Growth factors are thought to mediate this process (Nieuwkoop, 1992; Hogan et al., 1994). The dorsal vegetal cells (Nieuwkoop center) are the source of signals inducing dorsal mesoderm, which will give rise to notochord, prechordal plate and somites. Secreted molecules such as activin (Thomsen et al., 1990), Vg-1 (Thomsen and Melton, 1993) and several members of the *Wnt* family (Smith and Harland, 1991; Sokol et al., 1991) mimic this activity. Recent studies have suggested that specification of ventral mesoderm is also an active signaling process. A strong candidate for a ventral inducer, BMP-4 is expressed in ventroposterior tissues during development of both *Xenopus* and mouse (Jones et al., 1991; Fainsod et al., 1994; Hogan et al., 1994; Schmidt et al., 1995).

A Nieuwkoop center has not been identified for other vertebrates. However, the molecular events establishing dorsoventral polarity in teleost embryos might be similar to those described for *Xenopus* (reviewed by Driever, 1995). The Nieuwkoop center is thought to induce the Spemann organizer in the overlying dorsal marginal zone (Nieuwkoop, 1969; Kessler and Melton, 1994; Slack, 1994). The Spemann organizer defines a region of the gastrula that upon transplantation to the ventral side of an embryo induces secondary body axis, and thus is a source of signals that dorsalize paraxial mesoderm, as well as induce and pattern neural tissue. In the resulting secondary axis, the donor organizer tissue contributes predominantly to axial mesoderm: notochord and prechordal plate (Spemann, 1938). Functional equivalents of the *Xenopus* Spemann organizer have been identified by transplantation experiments in other vertebrates. These are the embryonic

shield in teleost fish (Oppenheimer, 1936; Ho, 1992), Hensen's node in the chick (Waddington, 1933) and the node in the mouse (Beddington, 1994). These regions in different vertebrate embryos share expression of a number of genes, including: *gsc*, *HNF-3β*, *Xlim-1*, *Xnot*, *noggin*, and *chordin* (reviewed by De Robertis et al., 1994).

Induction of neural tissue in ectoderm appears to occur in two ways: by vertical signaling from the invaginated axial mesoderm (Mangold, 1933) and by planar signals sent through the plane of ectoderm from the organizer (Kintner and Melton, 1987; Doniach et al., 1992; Sater et al., 1993). Dorsalizing and neuralizing signals emanating from the Spemann organizer like noggin (Lamb et al., 1993), chordin (Sasai et al., 1994; Holley et al., 1995) and follistatin (Hemmati-Brivanlou et al., 1994), might be counteracted or attenuated by molecules from the ventral signaling center, such as BMP-4 itself (Fainsod et al., 1994; Hogan et al., 1994; Holley et al., 1995).

Fate maps made at the beginning of gastrulation are comparable between vertebrates; the prospective axial mesoderm cells are located in the organizer region, and are usually the first to undertake movements creating the mesodermal germ layer. Somitic mesoderm is positioned laterally to axial mesoderm, while future ectoderm usually takes a more anterior position relative to mesoderm (Beddington and Smith, 1993). Furthermore, several types of gastrulation movements are common among vertebrates. During epiboly, the first morphogenetic movement in fish, frogs and chick, the blastoderm becomes thinner as its surface expands (Trinkaus, 1951; Keller, 1980; Schoenwolf, 1991). Germ layer formation in all vertebrates is characterized by involution or ingression movements that bring prospective mesodermal and endodermal cells to underlie the future ectoderm. Concurrently, the movements of convergence and extension cause both narrowing and extension of the embryonic body (Keller and Danilchik, 1988; Keller and Tibbetts, 1989). Finally, a still poorly understood set of cellular behaviors leads to formation of a tail bud and subsequently a tail (Gont et al., 1993; Catala et al., 1995). Although the cellular behaviors underlying some of these morphogenetic movements are well described, little is known about signals that direct gastrulation movements and how these signals are related to signals that control cell fate decisions (Keller et al., 1991).

Zebrafish (*Danio rerio*) is particularly well suited for studies of early development since in this system one can combine embryological and molecular methods with genetic analysis (Streisinger et al., 1981; Kimmel, 1989; Mullins et al., 1994; Solnica-Krezel et al., 1994). Here we report that in the course of a systematic mutagenesis screen for embryonic and early larval lethal mutations in zebrafish (Driever et al., 1996), we have identified a class of 25 mutations affecting specification of cell fates and cellular rearrangements during gastrulation. Complementation analysis indicated that the gastrulation mutations define at least 14 genetic loci. An initial characterization of mutant phenotypes has led to the classification of these mutations into three groups, based on their effects on cell fates in the gastrula. One class of mutants exhibits defects in dorsal structures, while the second class of mutants is deficient in ventral and posterior structures. Therefore the specifications of dorsal and ventral fates are controlled by separate genetic pathways. Furthermore, formation of ventral and posterior fates might require the same genetic components. Mutations of the third class interfere with cell rearrangements during gastrulation and have complex effects on the formation of cellular fates in the embryo. The identified mutations reveal relationships between the inductive and morphogenetic events during vertebrate gastrulation.

MATERIALS AND METHODS

F_2 screen

Methods for fish maintenance, mutagenesis, generating F_2 lines and general screening methods are described in Solnica-Krezel et al. (1994) and Driever et al. (1996). For the identification of gastrulation mutants the most important screening periods were at 6-12 hours post-fertilization (hpf) and at 24-30 hpf. All the crosses in which more than 10% of the embryos possessed consistent abnormalities at these stages, or approximately 25% of embryos were dead by 24-30 hpf, were repeated and the phenotypes of the resulting progeny analyzed during gastrulation and segmentation (5-24 hpf; Kimmel et al., 1995). F_2 fish that gave rise to phenotypically mutant progeny in both the primary and the secondary screens were outcrossed, and their sperm was preserved by freezing (Driever et al., 1996). Based on the phenotypes observed during the screen, 38 mutations were considered as potentially affecting gastrulation.

Recovery of gastrulation mutants from outcrosses

Mutations were recovered from the outcross lines by sibling crosses and visual inspection of the resulting progeny. Following the initial identification of the fish heterozygous for a given mutation, the cross was repeated and the resulting progeny was analyzed in detail at several stages of development. This analysis identified 23 mutations that lead to abnormally shaped gastrulae, caused deficiencies in specific cell types during gastrulation, or affected cell distribution. These mutants showed a characteristic set of morphological abnormalities at 24 hpf. Two additional mutants (*m472* and *m768*) exhibited normal morphology during gastrulation, but at 24 hpf developed defects similar to other gastrulation mutants. These 25 mutations were categorized as gastrulation mutants and analyzed further. From the remaining 13 mutations, three were recovered and after analysis included into different categories. We failed to recover ten mutations as zygotic recessive mutations. However, whether they can be recovered as maternal effect mutations remains to be tested.

Complementation analysis

Complementation was first tested between gastrulation mutants with similar phenotypes. This defined a smaller number of complementation groups, between which further allelism tests were performed. Additionally, complementation tests were performed between the gastrulation mutants and one mutation *hörnle* (*hör^{m274}*), which causes developmental arrest at 14/15 somite stage (Abdelilah et al., 1996). Finally, gastrulation mutations that lead to notochord and central nervous system (CNS) defects were tested for complementation with mutations from these two groups, respectively (Table 1; Schier et al., 1996; Stemple et al., 1996). For each complementation test a minimum of 30 fertilized eggs were obtained from crosses between identified heterozygous fish for any two given mutations. In the course of complementation analysis of the gastrulation mutations 157 successful crosses were performed, from which a total of 13,281 embryos (on average 85 per cross) were analyzed.

Phenotypic analysis of gastrulation mutants

Initial phenotypic characterization was performed for all mutations in this class. A more detailed analysis, described below, was applied to mutants representing ten loci not described previously. The following alleles of the described loci were analyzed: *oep^{m134}*, *boz^{m168}*, *unf^{m768}*, *cpt^{m52}* and *cpt^{m169}*, *gri^{m100}*, *ogo^{m60}*, *klu^{m472}*, *vol^{m712}*, *kny^{m119}*, *tri^{m209}*.

Table 1. Gastrulation mutants - summary

Genetic locus	Alleles	Phenotype	Other phenotypes		
Group I: Dorsal fates					
one-eyed-pinhead (oep)	*m134*	Prechordal plate missing. Cyclopia and ventral CNS deficiencies. Reduction of floor plate. Extension of the body axis reduced.	Body curved ventrally.	a, b	*
bozozok (boz) (Japanese: arrogant youth on motorcycles)	*m168*	Prechordal plate reduced. Chorda mesoderm missing. Cyclopia and ventral CNS deficiencies. Reduction of floor plate.		a, b	*
cyclops (cyc)	*m101, m122, m294*	Prechordal plate reduced. Cyclopia and ventral CNS deficiencies. Reduction of floor plate.	Body curved ventrally.	a,b,e	
uncle freddy (unf)	*m768*	Partial cyclopia. Cyclopia and ventral CNS deficiencies. Reduction of floor plate.	Body curved ventrally.	a,b	
floating head (flh)	*m614*	Lack of notochord. Floor plate reduced.		a, j	
no tail (ntl)	*m147, m550*	Notochord reduced and not differentiated. Tail reduced.		a, f	
Group II: Ventroposterior fates					
captain hook (*cpt*)	*m52, m169, m70 m282, m346, m586*	Reduction of ventral fin or progressive reduction of ventral and posterior tissues.	Craniofacial skeleton deficiencies (*m169*).	c, h	†
grinch (gri)	*m100*	Reduction of ventral fin fold and tail reduction and malformations.	Heart defects.		
ogon (ogo) (Polish: tail)	*m60*	Tail malformation, mulitple ventral finfolds formed. During gastrulation reduced convergence and abnormal tail morphogenesis.	Head malformations.	i	
kluska (*klu*) (Polish: noodle)	*m472*	Tail curved ventrally, infrequent variable ventral fin fold malformations.	CNS defects.		
Group III: Gastrulation movements (complex effects on cell fates)					
volcano (vol)	*m712*	Epiboly of the majority of deep cells arrested at the 60% stage.Blastoderm disintegrates at approximately 10 hours.	Early and rapid embryonic death.	d	
knypek (kny) (Polish: short)	*m119*	Reduced body length. Tail shorter and malformed. Rare partial cyclopia. During gastrulation reduced convergence and extension.	Notochord folded in the tail.	a	
trilobite (tri)	*m144, m209, m747 m778*	Reduced body length. Frequent partial cyclopia (*m209*). During gastrulation reduced convergence and extension. Low penetrance convergence and extension defect (*m778*)	Notochord folded in the tail. Low penetrance CNS degeneration (*m778*).	a	*
spadetail (spt)	*m423*	Lateral mesoderm fails to converge. Ectopic cells in the tail.	Pectoral fins missing.	g	

a, Stemple et al., 1996; b, Schier et al., 1996; c, Neuhauss et al., 1996; d, Abdelilah et al., 1996; e, Hatta et al., 1991; Hatta, 1992; f, Halpern et al., 1993; g, Kimmel et al., 1989; Ho and Kane, 1990; h, *m52* is an EMS-induced mutation; i, spontaneous mutation found in HK background; j, Talbot et al., 1995.

*Does not complement Tübingen mutant(s), name unified.

†*cpt*^{m52} does not complement or interacts with a mutant from Tübingen, name not unified.

Observation of live embryos

For phenotypic analysis of live mutant embryos, crosses were set up in the evenings between pairs of identified heterozygous fish. The next morning embryos were collected during the 1- to 64-cell stage of development, and subsequently sorted according to the number of cells, in order to ensure synchronous development. Embryos were cultured in egg water at 28.5°C, as described previously (Westerfield, 1994). Embryos were observed in chorions using a dissecting microscope (Wild M3 and M5). Alternatively, embryos were dechorionated manually and mounted in 1.5% solution of methyl cellulose in embryo medium on a bridge slide (bridge slides contained three layers of No. 2 cover slips, Westerfield, 1994) and viewed with Nomarski optics using a Zeiss Axiophot microscope. Detailed analyses of embryonic shape, cell distribution and formation of specific embryonic structures were performed at the following stages of development; dome (4.3 hpf), germ ring (5.5 hpf), shield (6 hpf), 75% epiboly (7.7 hpf), yolk plug closure (YPC, 9 hpf), tail bud (9.5 hpf), 10 somites (13.25 hpf), 26-30 hpf, 2-5 days post fertilization (dpf) (for description of these stages of development see Kimmel et al., 1995).

Whole-mount in situ hybridizations

These were performed essentially as described in Oxtoby and Jowett (1993). Antisense RNA probes were synthesized from cDNA encoding *axial* (Strähle et al., 1993), *gsc* (Schulte-Merker et al., 1992; Stachel et al., 1993), *eve1* (Joly et al., 1993), *sna1* (Hammerschmidt and Nüsslein-Volhard, 1993; Thisse et al., 1993), *ntl* (Schulte-Merker et al., 1994), *hlx1* (Fjose et al., 1994), *pax2* (Krauss et al., 1991; Püschel et al., 1992), *hgg1* (Thisse et al., 1994) and *myoD* (Weinberg et al., 1996).

Apoptic cell death

Apoptic cell death in fixed whole mounts was detected as described by Abdelilah et al. (1996).

Photography

Photography of live embryos was performed as described by Solnica-Krezel and Driever (1994). Stained embryos were cleared in glycerol. Single embryos were mounted in a drop of 100% glycerol on a bridge slide and photographed on the Axiophot microscope (Zeiss) on 160 ASA Ektachrome tungsten film. Images from photographic slides were scanned on a Kodak Professional RFs 2035 Plus Film Scanner. Composite figures were assembled, and contrast enhanced when necessary, using Adobe Photoshop (Adobe Corporation) software.

RESULTS

In a search for genes involved in vertebrate embryogenesis we performed a systematic chemical mutagenesis screen for recessive zygotic embryonic lethal mutations in zebrafish (Solnica-Krezel et al., 1994; Driever et al., 1996). To identify mutations affecting gastrulation, F_3 progeny of F_2 sibling crosses were screened for general morphological malformations at 6-12 hpf, and at 1 dpf. 25 mutations were identified that affect specification of cell fates and/or cell rearrangements during gastrulation. Here, we report on a genetic and phenotypic characterization of these mutations.

Genetic analysis of gastrulation mutants

Of the 25 identified mutations (Table 1), 22 are recessive. Among the recessive mutations, four are not fully penetrant: *bozozok*^{m168} (*boz*), *captain hook*^{m70} (*cpt*), *cpt*^{m282} and *cpt*^{m586}. Several mutations, particularly *boz*^{m168} and *uncle freddy*^{m768} (*unf*) show variable expressivity. Three mutations *cpt*^{m52}, *cpt*^{m169} and *cpt*^{m346} behave as semidominant mutations; in some crosses the progeny manifests the phenotype at a frequency higher than 25% (data not shown).

Complementation tests were performed between all of the gastrulation mutants, defining at least 14 complementation groups (Table 1). Four of these complementation groups correspond to previously known genes. We have identified three new alleles of the *cyclops* (*cyc*) gene (Hatta et al., 1991), two alleles of the *no tail* (*ntl*) gene (Halpern et al., 1993) and one allele of each of the *spadetail* (*spt*; Kimmel et al., 1989) and the *floating head* (*flh*) genes (Halpern et al., 1995; Talbot et al., 1995).

Effects of mutations on cell fates

Phenotypes of mutations representing the ten new loci were analyzed with respect to the effects on the formation of specific cell fates and on cell rearrangements during gastrulation. Based on this analysis, we classified the mutations into three groups: (1) mutations affecting formation of cell fates derived from the dorsal region of the zebrafish fate map; (2) mutations affecting predominantly ventral and posterior fates; and (3) mutations that alter cell rearrangements during gastrulation and have complex effects on cell fates in the gastrula (Table 1, Fig. 1).

Dorsal fates

Mutations in six loci, including the previously identified *cyc*, *flh* and *ntl*, lead predominantly to deficiencies in mesodermal and neuroectodermal cell fates derived from the dorsal region of the fate map (Fig. 1B-D). The axial mesoderm of zebrafish comprises anteriorly the prechordal plate, which gives rise to hatching gland and head mesoderm derivatives, and posteriorly chordamesoderm, which differentiates into notochord (Kimmel et al., 1995). The most severe defects in axial mesoderm are caused by the *boz*^{m168} mutation. On 1 dpf, *boz*^{m168} mutant embryos have a smaller body and exhibit variable deficiencies of the axial mesoderm (Fig. 1B). The most severely affected mutants lack the entire notochord. Furthermore, one of the derivatives of prechordal plate mesoderm, the hatching gland, is reduced or missing. Somites are fused in the midline and do not acquire the characteristic chevron shape. Mutants in the *oep*^{m134} gene are characterized by the lack of hatching gland cells and a

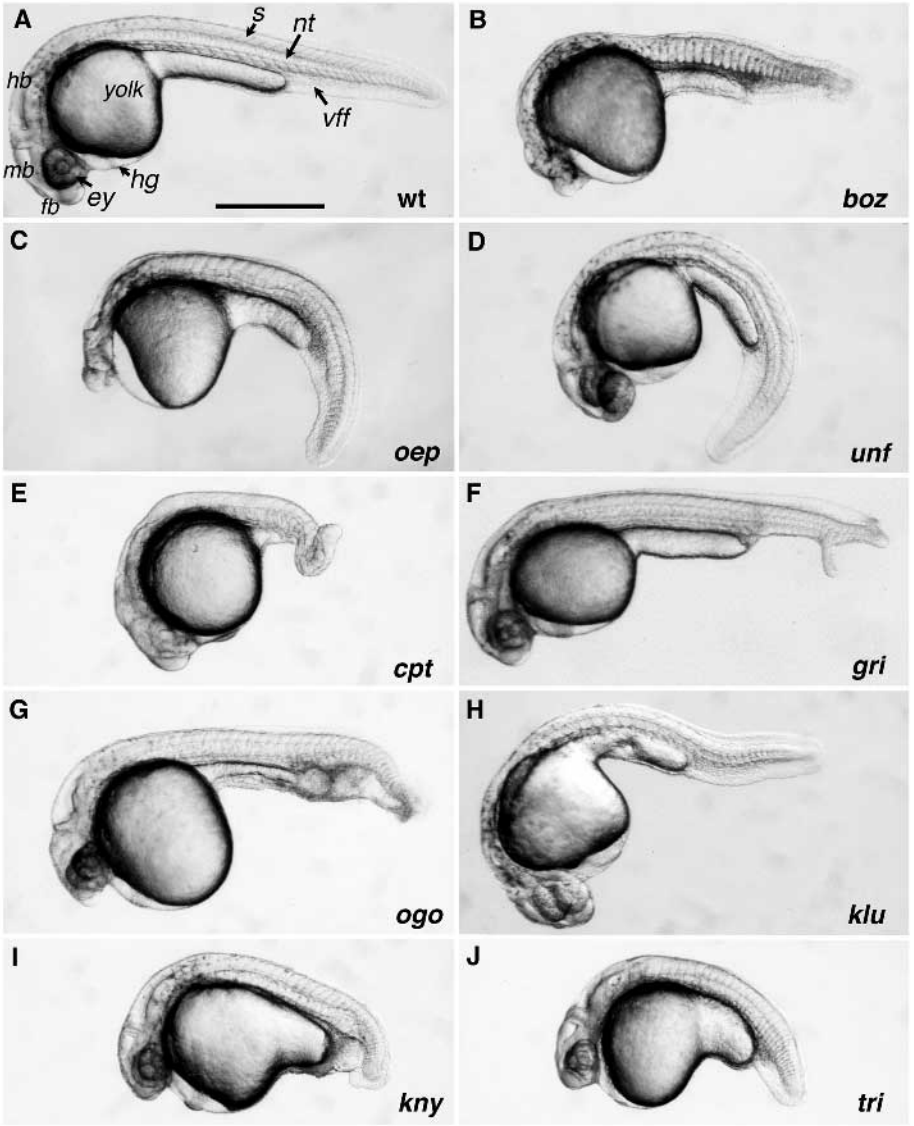

Fig. 1. The phenotypes of gastrulation mutants at day one of development. Dissecting microscope images of live embryos: (A) Wild type (wt); (B) *bozozok*^{m168}, (C) *one-eyed-pinhead*^{m134}, (D) *uncle freddy*^{m768}, (E) *captain hook*^{m52}, (F) *grinch*^{m100}, (G) *ogon*^{m60}, (H) *kluska*^{m472}, (I) *knypek*^{m119} and (J) *trilobite*^{m209} mutant embryos. *ey*, eye; *fb*, forebrain; *hb*, hindbrain; *hg*, hatching gland; *mb*, midbrain; *nt*, notochord; *vff*, ventral fin fold. Scale bar, 0.5 mm.

ventral curvature of the body. Notochord is present but frequently exhibits irregular morphology (Schier et al., unpublished data; Strähle et al., unpublished data) (Fig. 1C). *unf*^{m768} mutants also have a ventrally curved body (Fig. 1D). The notochord is bent, has abnormal cellular morphology, and is smaller in stronger phenotypes. Deficiencies in the formation of axial mesoderm in *boz*^{m168} and *oep*^{m134} mutant embryos can be detected at early stages of gastrulation (L. S.-K. and W. D., unpublished observation; A. F. S. and W. D., unpublished). At the tail bud stage, the expression of *gsc* in the prechordal plate region of the axial mesoderm is reduced in *boz*^{m168} embryos, and appears to be totally absent in the neuroectoderm (Fig. 2A,B). At this stage of development *oep*^{m134} mutants also exhibit deficiencies in the most anterior dorsal mesoderm. This is revealed by the absence of a polster, a characteristic thickening of the hypoblast underlying the anterior-most neural plate (Fig. 3B) (Kimmel et al., 1995). Furthermore, *boz*^{m168} (but not *oep*^{m134}) embryos exhibit a total absence of the *ntl* RNA in the chordamesoderm region, while expression of this gene in the blastoderm margin is not affected (Fig. 2A,B).

Most of the dorsal fate mutants are also characterized by deficiencies in ventral CNS structures, reminiscent of defects described previously for mutations in the *cyc* gene (Hatta et al., 1991, 1994; Hatta, 1992). They show a variable degree of cyclopia, from eyes positioned closer to one another in *unf*^{m768}, to one eye, or very reduced/absent eyes in *oep*^{m134} and *boz*^{m168} (see also Schier et al., 1995). The ventralmost part of the spinal cord, the floor plate, is partially (*unf*^{m768}) or almost completely missing (*oep*^{m134} and *boz*^{m168}). Finally, ventral aspects of the forebrain and midbrain are severely reduced, as shown for *boz*^{m168} mutant embryos by the absence of *hlx1* gene expression in the diencephalon (Fig. 2C,D).

Less pronounced deficiencies in ventral aspects of the CNS are caused by another class of mutations. *trilobite* (*tri*) and to a lesser extent *knypek* (*kny*) mutants exhibit, with low penetrance and variable expressivity, reduced spacing between the eyes or partial cyclopia at 1 dpf (data not shown). *tri*^{m209} mutant embryos exhibit a compressed expression domain of *shh* in ventral brain (Fig. 2E,F).

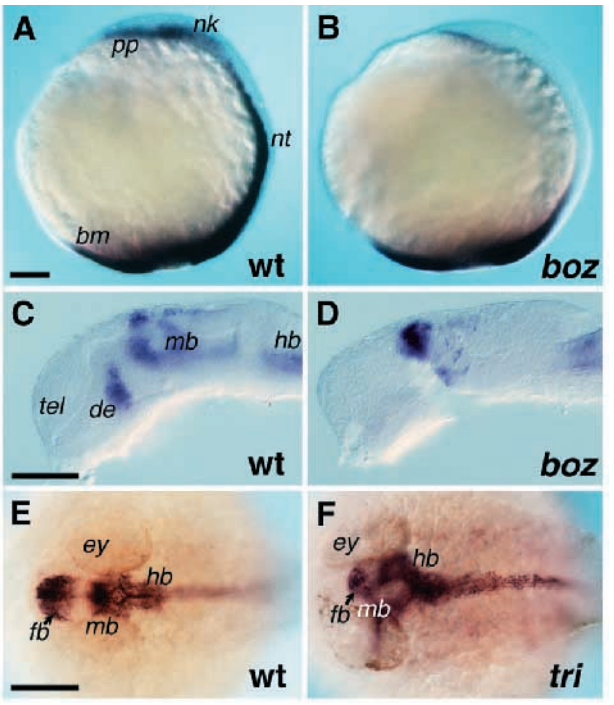

Fig. 2. Expression patterns of cell type and region-specific genes during development of mutants affecting dorsal fates. (A,B) Expression of *gsc* and *ntl* RNA in wild-type (wt) (A) and *boz*^{m168} (B) mutant embryos at the bud stage (9.5 hpf). *pp*, *gsc* expression domain in prechordal plate; *nk*, *gsc* expression domain in neural keel; *nt*, *ntl* expression domain in chordamesoderm; *bm*, *ntl* expression domain in the blastoderm margin. (C,D) Expression pattern of *hlx1* RNA in wild-type (C) and *boz*^{m168} mutant embryos at 30 hpf; *de*, *mb*, expression domain in diencephalon and midbrain, respectively. (E,F) Expression of *shh* RNA in wild-type (E) and *tri*^{m209} mutant embryo at 30 hpf. *ey*, eye; *fb*, forebrain; *hb*, hindbrain; *mb*, midbrain. Scale bar, 0.1 mm.

Ventral and posterior fates

Nine mutations in four complementation groups lead to deficiencies in and/or malformations of ventral and posterior structures in the embryo. The *cpt* complementation group consists of six mutations (*m52, m70, m169, m282, m346, m586*; Table 1). The weakest alleles are characterized by lack or reduction of the ventral fin fold (not shown). The stronger alleles (*cpt*^{m52}, *cpt*^{m169}) manifest tail truncations of a variable degree (Figs 1E 5C). The somite number is reduced and the caudal vein is truncated posteriorly. However, blood cells form in *cpt* mutant embryos. Another frequent malformation of the tail in *cpt*^{m52} and *cpt*^{m169} mutants is a triple fin fold arrangement (Fig. 5E).

Several observations indicate that the *cpt* complementation group might include mutations affecting more than one locus. First, in addition to tail deficiencies, *cpt*^{m169} mutant embryos exhibit craniofacial defects (Table 1; described by Neuhauss et al., 1996), while *cpt*^{m52} mutants in some crosses are characterized by a reduced and malformed head (data not shown). The *cpt*^{m52}/*cpt*^{m169} transheterozygotes do not exhibit craniofacial defects, and the tail reduction is less pronounced than in the homozygotes for either mutation. Therefore the transheterozygote phenotype might reflect a genetic interaction between non-allelic mutations, rather than non-complementation of two mutations in the same locus. Finally, in some genetic backgrounds the *cpt*^{m52} mutation is semidominant, making complementation tests difficult to interpret.

cpt^{m52} mutant embryos distinguish themselves at the tail bud stage. They are abnormally elongated in the animal-vegetal axis and exhibit a misshapen tail bud (Fig. 3C). Subsequently, the extending tail everts prematurely, and Kupffer's vesicle becomes dislocated from the yolk in the *cpt*^{m52} mutant embryos (Fig. 4B). Kupffer's vesicle is a transient structure normally located midventrally in the distal part of the forming tail and positioned close to the yolk cell in the wild-type embryo (Fig. 4A; Kimmel et al., 1995). As extension continues, the tail in *cpt* mutant embryos becomes folded. This leads to fusions along the ventral (*cpt*^{m169}, Fig. 5C) or dorsal tail surfaces (*cpt*^{m52}, Fig. 1E). The observed deficiencies in the ventroposterior structures of the *cpt* mutant embryos may reflect defects in specification of ventral fates. Consistent with this idea, *cpt*^{m169} mutant embryos exhibit a decrease in the expression of the ventroposterior marker *eve1* in the developing tail (Fig. 6A,B) (Joly et al., 1993). In contrast, the expression domain of

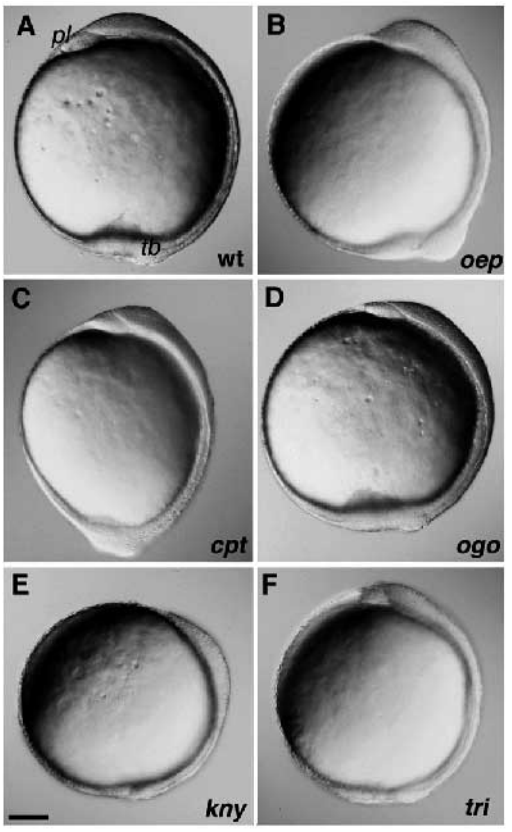

Fig. 3. Morphology of selected gastrulation mutants at the tail bud stage of development (9.5 hpf). Nomarski images of live embryos. (A) Wild type (wt); (B) *oep*^{m134}, (C) *cpt*^{m52}, (D) *ogo*^{m60}, (E) *kny*^{m119} and (F) *tri*^{m209} mutant embryos. *pl*, polster; *tb*, tail bud. Anterior is towards the top, and dorsal towards the right. Scale bar, 0.1 mm.

the dorsolateral somitic marker *myoD* (Weinberg et al., 1996), becomes expanded ventrally, and in the posteriormost somites spreads also to ventral positions (Fig. 6C-F).

A mutation in a different locus, *grinch*^{m100} (*gri*^{m100}), leads to a similar but less pronounced gastrulation phenotype (Fig. 4C,F), and is manifest at 1 dpf by deficiencies in the ventro-posterior portions of the tail. These deficiencies are often accompanied by formation of ectopic protrusions from the ventral aspect of the tail (Fig. 1F). Fig. 5B shows that in the tail of *gri*^{m100} mutant embryos the ventralmost cell types, ventral fin fold and caudal vein, are missing.

Tail reduction phenotypes are also exhibited by *kny*^{m119} and *tri*^{m209} mutant embryos in which convergence and extension are affected (Fig. 1I,J). In contrast to *cpt*^{m52} and *gri*^{m100} mutants, the somite number is not reduced. Expression of the *eve1* gene is normal in *tri*^{m209} mutants (data not shown). In contrast, *kny*^{m119} mutant embryos exhibit an ectopic expression of *eve1* in a group of ventral cells in the anus region, in addition to the normal domain of expression of this gene in the most posterior part of the tail (Fig. 9G,H). An abnormal accumulation of cells in this region is also seen in living embryos (Fig. 1I).

A distinct set of defects in the ventral tail is observed in *ogon*^{m60} (*ogo*^{m60}) mutants. At 1 dpf the tail is shorter and enlarged in the ventral region near the anus, where an abnormal accumulation of cells is observed (Fig. 1G). The ventral fin fold is malformed, and frequently multiple fin folds are present at the tip of the tail (Fig. 5F,G). Furthermore, *ogo*^{m60} mutant embryos develop a reduced head with enlarged brain ventricles (Fig. 1G). At the tail bud stage the *ogo*^{m60} mutants exhibit a shortened anterior-posterior axis and a small tail bud (Fig. 3D). At the 10 somite stage, however *ogo*^{m60} mutants have a very distinct morphology: the embryonic body is shortened, the forming tail is abnormally shaped and ectopic accumulation of cells is seen ventral to the tail (Fig. 4G). This region contains an increased number of apoptotic cells, as revealed by an assay for fragmented DNA (Fig. 7G,H) (Zekeri et al., 1993). Furthermore, the expression domain of *eve1* appears enlarged in the *ogo*^{m60} mutants (Fig. 7E,F). It is not clear whether this is due to an increase in the number of cells expressing this gene, or to an abnormal distribution of a normal number of such cells.

Effects of mutations on cellular rearrangements

In zebrafish, at least three major types of cell rearrangements shape the embryo during gastrulation: epiboly, involution/ingression and convergence and extension (Warga and Kimmel, 1990; Kane and Warga, 1994; Solnica-Krezel et al., 1995). Most of the mutants described above and in the following section exhibit an abnormal morphology during gastrulation (Figs 3 and 4). To determine which morphogenetic processes are affected in these mutants, we analyzed changes in shapes of the embryos during gastrulation, distribution of distinct cell types in living embryos and patterns of expression of region-specific markers by in situ hybridization. Our analysis indicates that several of the mutations affect distinct cellular rearrangements during gastrulation.

Epiboly

Epiboly is the first morphogenetic movement during zebrafish embryogenesis (Warga and Kimmel, 1990; Wilson et al., 1995). It involves expansion of all three cell types of the blastula: yolk syncytial layer (YSL), enveloping layer (EVL) and deep cell layer, towards the vegetal pole (Trinkaus, 1984b; Solnica-Krezel and Driever, 1994). The mutation *volcano*^{m712} (*vol*) appears to interfere with this process (Table 1). The *vol*^{m712} phenotype becomes apparent when the blastoderm of wild-type embryos covers 70% of the yolk cell. At the same time, in *vol*^{m712} mutant siblings, the blastoderm covers only approximately 60% of the yolk sphere. While in wild-type embryos epiboly continues finally to close the yolk plug at 9 hpf, only a very slow vegetal expansion of the blastoderm is observed in mutant embryos (Fig. 8A,B). Closer observation indicates that, while epiboly of the majority of deep cells is affected in the mutant embryos, epibolic expansion of the yolk syncytial nuclei and of the superficial EVL continue at the wild-type or slightly reduced rates. Furthermore, a small group of deep cells located on the dorsal side of the embryo, dorsal forerunner cells (Hammerschmidt and Nüsslein-Volhard, 1993), are also found close to the vegetal pole, far ahead of the remaining deep cells (Fig. 8E,F). These observations are supported by analysis of expression of the *gsc* and *ntl* genes. At 90% epiboly, in wild-type embryos *ntl* RNA is expressed in three domains: chordamesoderm, blastoderm margin and dorsal forerunner cells (Fig. 8C,G) (Schulte-Merker et al., 1992, 1994). In sibling mutant embryos the *ntl* blastoderm margin expression domain

is located at a larger distance from the vegetal pole. However, the dorsal forerunner expression domain is located close to the vegetal pole, similar to wild-type embryos (Fig. 8D,H). Interestingly, the *gsc* expression domain extends as far anteriorly as in the wild-type embryo, indicating that the anterior ward migration of the hypoblast is not significantly affected by the *vol*^{m712} mutation (Fig. 8C,D). In contrast, the chordamesoderm expression of *ntl*, and the expression domain of the *axial* gene in dorsal hypoblast, are less extended and wider than in wild type (Fig. 8G,H,K,L). Starting at 9 hpf, some cells of the EVL in *vol*^{m712} mutant embryos become round (Fig. 8I). Subsequently, the blastoderm of the mutant embryos disintegrates (Fig. 8J) and finally the yolk cell ruptures. No evidence of excessive cell death was found in mutant embryos at the time when some of the mutants were already disintegrated (not shown). Furthermore, incubation of embryos in isotonic buffers prolongs survival of the mutants for several hours. Although some morphogenetic processes (somitogenesis, eye development) are initiated in these mutant embryos, epiboly is never completed (data not shown).

Convergence and extension

In teleost fish, convergence of cells from ventral and lateral positions toward the dorsal side of the yolk cell leads to thickening of the embryonic shield. Subsequently, convergence and extension movements involving mediolateral cell intercalations drive both narrowing and extension of the embryonic axis in the anterior-posterior (AP) direction (Warga and Kimmel, 1990; Trinkaus et al., 1992). Progress of convergence and extension is manifested by shape changes of the entire embryo, from spherical at the 50% epiboly stage, to an oval shape at the end of epiboly. Notochord, somites and neural plate narrow along the mediolateral axis while elongating in the AP direction (Kimmel et al., 1995). Furthermore, expression domains of various cell type specific genes undergo characteristic changes due to convergence and extension; they move toward the dorsal midline, or narrow in the mediolateral direction and become elongated in the AP direction.

Several mutations identified in the screen interfere with the extension of the embryonic axis during gastrulation. As described above, *vol*^{m712} mutants show a decrease in extension as well as some decrease in convergence (Fig. 8). Further, mutants from four complementation groups, *oep*^{m134}, *ogo*^{m60}, *kny*^{m119} and *tri*^{m209}, have a shorter embryonic body rudiment at the tail bud (Fig. 3B,D,E,F) and 10 somite stages (Fig. 4G-L). At 1 dpf, these mutants exhibit a reduction of body length, which is most severe for *kny*^{m119} and *tri*^{m209} (Fig. 1).

Several observations indicate that in the case of the latter two mutants, defects in the extension are accompanied by decreased dorsal convergence. First, the dorsal view of these two mutants at the 10 somite stage reveals that somites and neural keel are not only less extended along the AP axis than in wild-type embryos, but also wider (less converged) along the mediolateral axis (Fig. 4H,I,K,L). The expression domains of *pax2* in the midbrain anlage (Krauss et al., 1991; Püschel et al., 1992), of *hlx1* in the prechordal plate region (Fjose et al., 1994) and of *myoD* in the forming somites (Weinberg et al., 1996) are less extended in the AP direction and less converged in the dorsolateral direction (Fig. 9A,B,E,F). Further, the longitudinal stripes of *pax2* RNA that mark future pronephros and converge toward the dorsal axis during gastrulation are located more laterally in *tri*^{m209} mutant embryos (Fig. 9C,D). It will be important to ask whether the delayed dorsal convergence of domains of gene expression in these mutants does indeed reflect abnormalities in movements of cells expressing those genes. In contrast, in the *ogo*^{m60} mutant embryos at the 10 somite stage, somites do not show a significant reduction of convergence (Fig. 4J). The pattern of expression of the *myoD* RNA in forming somites confirms that extension, but not convergence is affected; somites exhibit normal width but are packed closer together and are shorter along the AP axis (Fig. 7A-D).

DISCUSSION

We have found 25 mutations affecting specification of cell

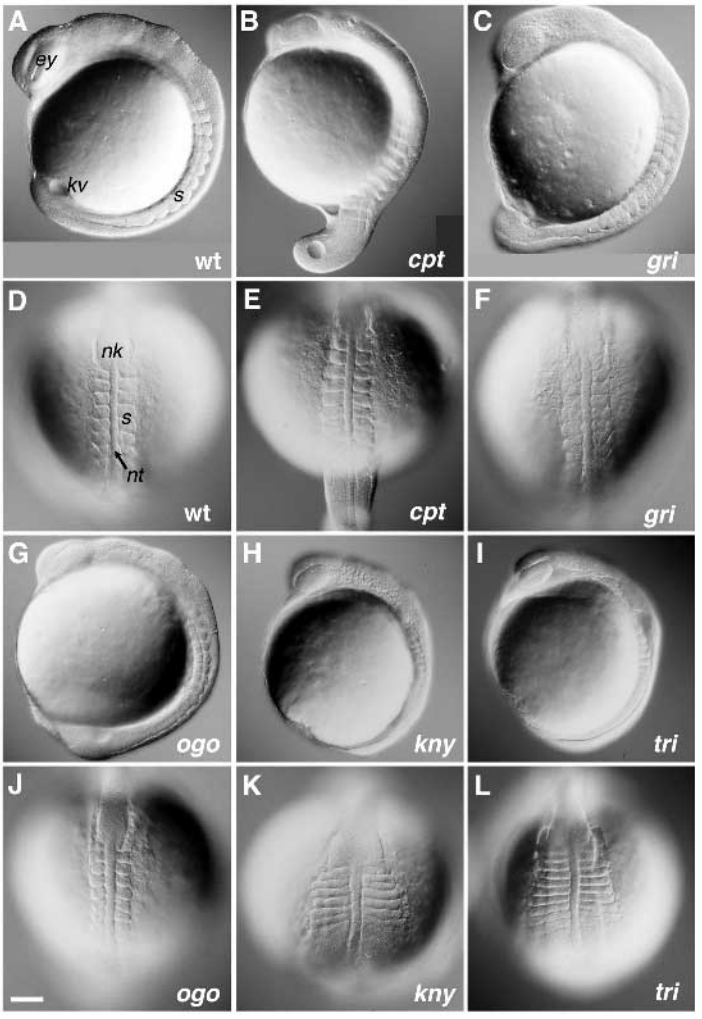

Fig. 4. Morphology of selected gastrulation mutants at the 10 somite stage (13.25 hpf). Nomarski images of live embryos. (A-C,G-I) Lateral views, anterior is to the top and dorsal towards the right. (D-F,J-L) Dorsal views, anterior is towards the top. (A,D) Wild type (wt); (B,E) *cpt*^{m52}, (C,F) *gri*^{m100}, (G,J) *ogo*^{m60}, (H,K) *kny*^{m119} and (I,L) *tri*^{m209} mutant embryos. *ey*, eye; *nk*, neural keel; *nt*, notochord; *s*, somite, *kv*, Kupffer's vesicle. Scale bar, 0.1 mm.

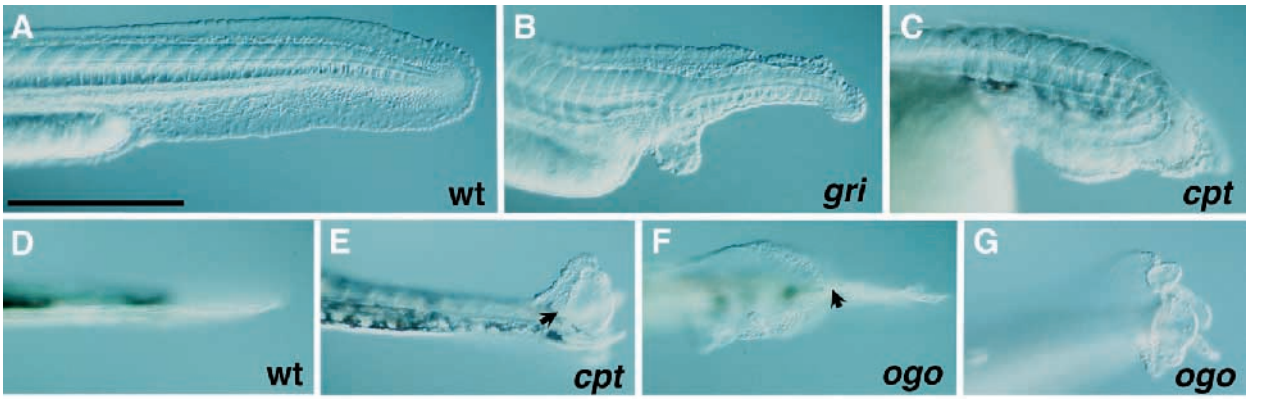

Fig. 5. Different types of tail malformations in the mutants affecting ventroposterior fates. (A-C) Lateral views at 1 dpf, anterior towards the left, dorsal towards the top. (D-G) Ventral views at 3 dpf, anterior is towards the left. (A,D) Wild type (wt); (B) *grinch*^{m100}, (C,E) *cpt*^{m169} and (F,G) *ogo*^{m60} mutant embryos. E and F show the triple fin fold morphology frequently observed in *cpt* and *ogo* mutants. In wild type (D), the ventral fin fold (positioned perpendicularly to the plane of the figure) has only a single edge. In contrast, in the mutant embryos a portion of the ventral fin fold becomes flattened (with the flattened surface parallel to the plane of the figure, while the dorsal fin fold remains perpendicular to it) and forms two edges. When the two edges of the ventral fin fold meet a single edge of the dorsal fin fold (arrow), the triple fin fold arrangement is created. Scale bar, 0.5 mm.

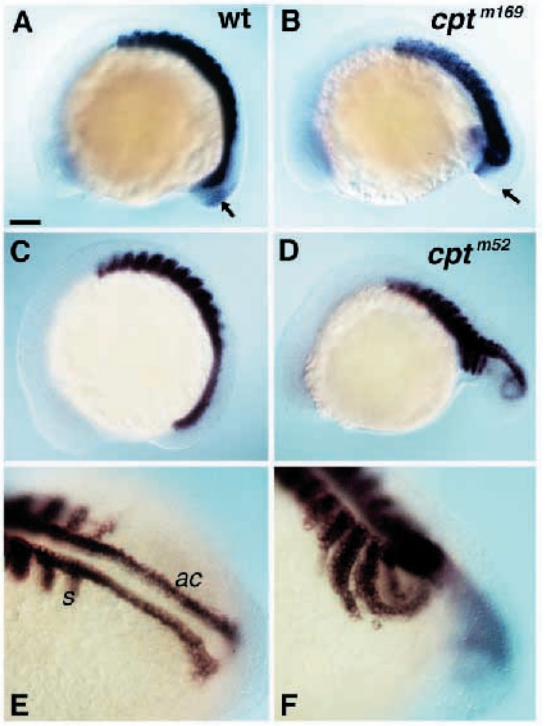

Fig. 6. Decrease in the expression of ventroposterior marker *eve1*, and lateral expansion of a somitic marker *myoD* in *cpt* mutant embryos during somitogenesis. (A,C,E) Wild type (wt); (B) *cpt*^{m169} and (D,F) *cpt*^{m52} mutant embryos. (A,B) Expression of *myoD* and *eve1*, *eve1* expression domain in the tail is indicated by an arrow. (C-F) Expression of *myoD* mRNA. (A-D) Lateral views, anterior towards the left and dorsal towards the top; (E,F) Dorsolateral view of developing tail. *s*, somites; *ac*, adaxial cells. Scale bar, 0.1 mm.

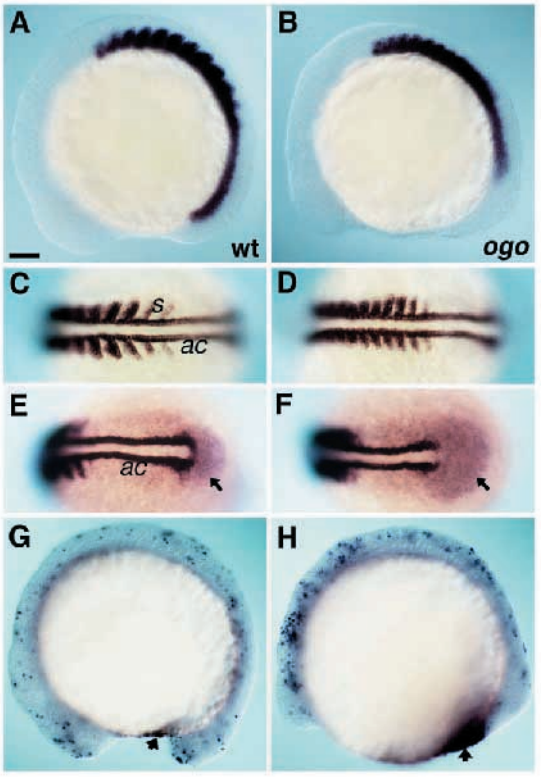

Fig. 7. Expression patterns of cell type and region-specific genes at the 10 somite stage in *ogo*^{m60} mutants affected in formation of ventral and posterior fates. (A,C,E) Wild type (wt); (B,D,F) *ogo*^{m60} mutant emryo. (A-D) In situ hybridization of *myoD* mRNA; (E,F) Expression of *myoD* and *eve1* mRNA (arrow). (G,H) Visualization of dying cells in *ogo*^{m60} mutants at the 13 somite stage. A ventral region with increased numbers of dying cells is indicated by an arrow. (G,H) Detection of apoptotic cells in wild-type (G) and *ogo* (H) mutant embryos at the 13 somite stage. Arrow indicates a region with increased number of dying cells. (A,B) Lateral views, anterior towards the left and dorsal towards the top; (C,D) Dorsal view; (E,F) Dorsoposterior view. *s*, somites, *ac*, adaxial cells. Scale bar, 0.1 mm.

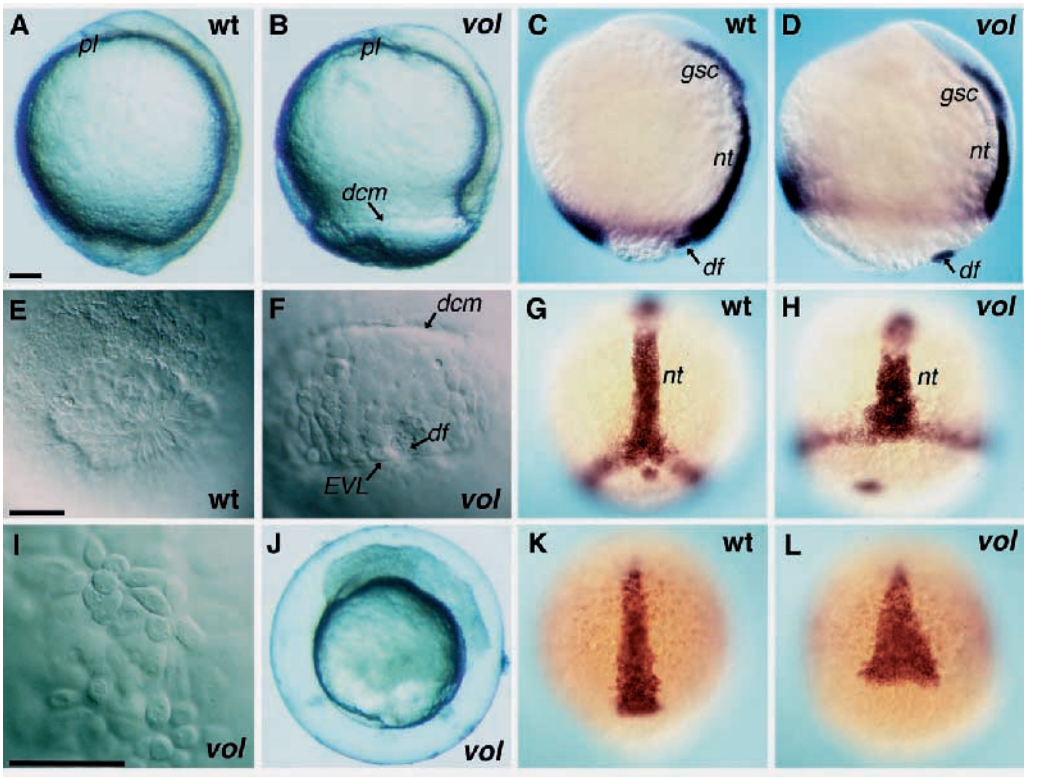

Fig. 8. Changes in cellular rearrangements and patterns of gene expression during development of the *vol*^{m712} mutants. (A,C,E,G,K) Wild type (wt); (B,D,F,H,I,J,L) *vol*^{m712} mutant embryo. (A,B) Dissecting microscope images at the tail bud stage. Lateral view, dorsal toward the right. (E,F,I) Nomarski images at the tail bud stage, 30 minutes after the yolk plug closure in wild-type embryos. *pl*, polster; *dcm*, margin of deep cells; *df*, dorsal forerunner cells. (J) Dissecting microscope image of a *vol*^{m712} mutant embryo at 10 hours. Embryo is in chorion, blastoderm is disintegrating. (C,D,G,H) Expression of *gsc* and *ntl* mRNA at 90% epiboly. (K,L) Expression of *axial* mRNA at 90% epiboly. *nt*, notochord expression domain of *ntl*; *df*, dorsal forerunner expression domain of *ntl*. Scale bars, 0.1 mm.

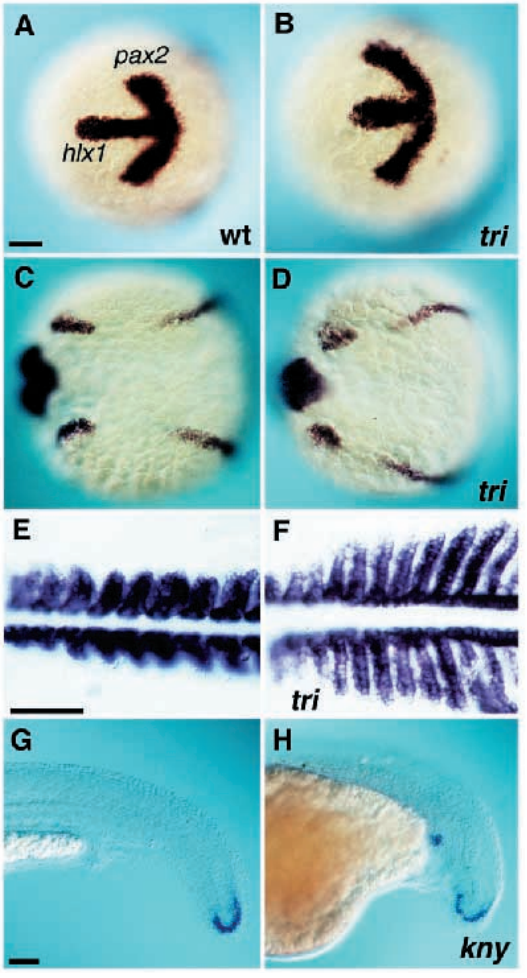

fates and/or cellular rearrangements during gastrulation in zebrafish. The mutations define at least 14 complementation groups, with an average of 1.8 alleles per group. The number of identified loci might be greater given that the *cpt* complementation group may contain mutations in more than one locus, masked by semidominant behavior of some *cpt* alleles. This issue will be unequivocally resolved by mapping these mutations, and this is currently in progress (Knapik et al., 1996). Since ten complementation groups contain one allele each, only a fraction of all genes that mutate to visible gastrulation defects has been isolated in this screen (Driever et al., 1996). Nevertheless, new alleles have been identified for all previously described zebrafish gastrulation genes; *cyc* (Hatta et al., 1991), *ntl* (Halpern et al., 1993), *spt* (Kimmel et al., 1989) and *flh* (Halpern et al., 1995; Talbot et al., 1995). Since the F_2 genetic screen was designed to recover zygotically acting recessive embryonic lethal mutations (Driever et al., 1996), certain classes of developmental genes were excluded from the screen. Fully penetrant dominant-lethal mutations would be manifested and eliminated in the F_1 generation. Low-penetrance dominant mutations would also have a lower probability of recovery. This is an important consideration, since mice heterozygous for a targeted deletion in the *HNF3β* gene

Fig. 9. Changes in expression patterns of cell type and region-specific genes in mutants affected in convergence and extension. (A,C,E,G) Wild type (wt); (B,D,F) *tri*^{m209} and (H) *kny*^{m119} mutant embryos. (A,B) Expression of *hlx1* and *pax2* mRNA at the tail bud stage, view of developing head region. Anterior is towards the left. (C,D) Expression of *pax2* at the tail bud stage. Dorsal view. (E,F) Expression of *myoD* mRNA at the 10 somite stage. Dorsal view, anterior toward the left. (G,H) Expression of *eve1* mRNA in tail at 1 dpf. Note ectopic expression in the mutant embryo. Scale bar, 0.1 mm.

exhibit a low penetrance mutant phenotype that decreases their survival (Ang and Rossant, 1994; Weinstein et al., 1994). Another set of mutations that is not represented in this screen is recessive maternal effect mutations, which would be seen only in the progeny of F_3 females. A number of genes that function during early vertebrate development are contributed maternally, e.g. *Vg-1*, *Xwnt-11* (Kessler and Melton, 1994). Mutations in such genes would not be likely to be identified in our screen.

Phenotypic analysis defined three classes of mutations with respect to their effect on embryonic pattern formation. The first class of mutations affects specification of dorsal fates in the embryo, while the second class interferes with specification of ventroposterior fates. Therefore, dorsal and ventral fates in the embryo are controlled by separate genetic pathways. Mutations in the third class affect primarily cell rearrangements during gastrulation and have complex effects on cell fates. Morphogenetic processes are also affected by some mutations from the first two groups. Therefore, cell rearrangements during gastrulation are dependent both on the genes that control cell fates and on separate genetic pathways.

Genetics of gastrulation movements

Mutations in eight new loci interfere with cell rearrangements during gastrulation. Some mutations, e.g. *boz* and *oep*, *cpt*, *gri* might initially lead to changes in specification of cell fates or in embryonic polarity before or during gastrulation. In such cases abnormalities in cellular rearrangements in these mutants might be a consequence of altered cellular fates. For *kny* or *tri* mutants we have not detected any changes in the expression of dorsal and ventral markers prior to gastrulation. Therefore the gastrulation defects observed in these mutants might reflect an inability of cells to interpret the normal positional information, or to execute the morphogenetic program.

Morphogenetic changes during gastrulation are brought about by a number of cellular activities. These include directional cell movement, cell intercalation, cell shape changes, expansion and decrease of a surface area and cell proliferation (Trinkaus, 1984a; Keller et al., 1991). Our analysis of the gastrulation mutants clearly shows that cell rearrangements and morphogenetic changes during gastrulation are abnormal. Further work should reveal whether the cellular movements themselves or other specific cellular activities are affected.

Epiboly

Epiboly is the first morphogenetic movement involving vegetal expansion of the deep cell layer, the enveloping layer (EVL) and the yolk syncytial layer (YSL; reviewed by Trinkaus, 1984b; Solnica-Krezel et al., 1995). In vol^{m712} mutants, epiboly of the majority of deep cells is arrested when the blastoderm covers 60% of the yolk cell. However, the yolk syncytial nuclei, the EVL and a small group of dorsal forerunner deep cells, continue to undergo epiboly, until the blastoderm disintegrates at about the 10 hpf. The vol^{m712} phenotype indicates that the mechanism of epiboly of the EVL and deep dorsal forerunner cells is independent of the epiboly of the remaining deep cells. The fact that epiboly of only a subset of cells is affected would argue against the phenotype being the simple consequence of a generally reduced cellular viability or motility. One caveat is that the epibolic expansion of the EVL is thought to be passive and driven by the expansion of the YSL surface to which the EVL is attached (Trinkaus, 1951, 1984b). Therefore, it will be important to determine whether in mutant embryos the dorsal forerunner cells do actively migrate towards the vegetal pole, or are passively carried on the expanding surface of the YSL (or EVL).

The uncoupling of epiboly of EVL from epiboly of deep cells and yolk syncytial nuclei was observed when microtubules were disrupted (Solnica-Krezel and Driever, 1994). However, the vol^{m712} phenotype demonstrates for the first time a heterogeneity with respect to epibolic movements within the deep cell population. Furthermore, epiboly of the YSL is not sufficient for the epibolic expansion of the majority of deep cells (Trinkaus, 1951).

Convergence and extension

We found mutations in five loci that lead to reduction in the extension of the embryonic axis. In teleost fish, convergence of at least a part of the hypoblast is driven by directional migration of more ventrally located cells towards the embryonic shield. It is mainly in the more dorsal positions where mediolateral intercalations occur (Trinkaus et al., 1992). As in frogs, mediolateral intercalation leads to narrowing and extension of the embryonic axis (Keller and Tibbetts, 1989; Warga and Kimmel, 1990; Shih and Keller, 1992). In fish and in frogs epiboly also contributes to extension.

The most dramatic extension defect is observed for kny^{m119} and tri^{m209} mutants. Both convergence and extension are affected. The decrease in extension could be a consequence of the defect in convergence, since a smaller number of cells is present on the dorsal side where the mediolateral intercalations mainly occur. Alternatively, slower extension might reflect a requirement for functions of those genes in both directional migration of cells (convergence) and in mediolateral intercalation. Indeed, in the *spt* mutant, while a large number of cells from lateral mesoderm fail to converge (Kimmel et al., 1989; Ho and Kane, 1990), chordamesoderm nevertheless converges and extends, and the overall extension defect is less pronounced than in the *kny* and *tri* mutants.

A decrease in extension and convergence is also observed in the vol^{m712} mutants, and may be a direct consequence of the arrested vegetal ward epibolic expansion of the blastoderm. This is consistent with the idea that epiboly does contribute to extension (Wilson and Keller, 1991). In contrast, for oep^{m134} and ogo^{m60}, reduction in extension does not correlate with an obvious decrease in convergence, or in epiboly. Other defects could lead to a reduced extension. Firstly, the number of cells in the embryo could be reduced due to a proliferation defect. Secondly, mediolateral intercalation could be affected. Finally, a more elongated oval shape of the cpt^{m52} mutant embryos at the bud stage might result from an increase in convergence and/or extension.

Tail forming movements

The nature of cell movements and patterning events involved in tail morphogenesis in vertebrates is poorly understood. Recent studies in frog and chick embryos indicate that the tail bud consists of distinct cell populations (Gont et al., 1993; Catala et al., 1995; Tucker and Slack, 1995). Furthermore, cell intercalation (Gont et al., 1993), invagination and divergence

occur during tail morphogenesis (Catala et al., 1995). Tail formation is affected in several mutants described here. Mutations in the genes *kny* and *tri*, result in decreased convergence and extension, producing a shorter and wider tail. The *ogo*^{m60} mutants exhibit an abnormally shaped tail bud, as well as abnormal morphology of the tail. Finally, the *cpt* and *gri* mutations lead to premature eversion of the tail from the yolk cell. Preliminary cinematographic analysis indicates that cell movements in the tail bud of the *cpt*^{m52} mutants differ from those observed in the wild type (E. M.-S. and W. D., unpublished observations). It is noteworthy that, with the exception of *tri* and *ntl*, all the remaining mutations affecting tail morphogenesis also affect the formation of ventroposterior fates in the embryo. Further studies should explain the nature of abnormal cell movements in this group of mutants, and the relationship between tail morphogenesis and signals inducing embryonic polarity.

Genetics of embryonic polarity

The analysis of the mutant phenotypes defines two groups of mutations, according to their effects on the formation of cell fates in the embryo.

Dorsal fates

The first group of mutations affects six loci: *oep*^{m134}, *boz*^{m168}, *unf*^{m768} (including the previously identified *cyc*) (Hatta et al., 1991), *flh* (Halpern et al., 1995) and *ntl* (Halpern et al., 1993). These mutations lead to defects in the formation of dorsal mesodermal structures, notochord and/or prechordal plate, and in ventral aspects of the CNS. During zebrafish development, cellular fates can be predicted on the basis of position within the embryo at the late blastula stage (50% epiboly) (Kimmel et al., 1990). On this fate map, cells that will give rise to notochord and prechordal plate are located in the dorsalmost marginal positions (Kimmel et al., 1995). In this region the organizer-specific gene *gsc* is expressed (Stachel et al., 1993; Schulte-Merker et al., 1994) and the embryonic shield, the fish gastrula organizer, will form (Warga and Kimmel, 1990; Ho, 1992). Since mutations from this group also affect expression of the organizer-specific genes (Thisse et al., 1994; Talbot et al., 1995), they are likely to be involved in the formation, maintenance or function of the organizer. Consistent with this idea, some mutants in this group exhibit defects in patterning of the neuroectoderm, partial or complete cyclopia, reduction of the eyes, and deficiencies in the ventral structures of the CNS. This combination of defects resembles abnormalities displayed by experimentally ventralized *Xenopus* embryos (Scharf and Gerhart, 1983). Partially ventralized embryos with dorsoanterior index (DAI) 3 and 4 exhibit cyclopia or eye reduction, respectively, and reduction of anterior brain structures (Kao and Elinson, 1988). These phenotypes are comparable to those caused by mutations in *oep*, *unf* and *cyc* loci (Hatta et al., 1991). More ventralized *Xenopus* embryos with DAI 2 also exhibit the loss of notochord (Scharf and Gerhart, 1983), resembling the *boz* mutant phenotype. Therefore mutations described here are likely to identify components of the pathway(s) affected by the ventralizing treatments.

Mutant mice homozygous for a targeted deletion of one of the genes expressed in the gastrula organizer, *HNF-3β*, lack notochord and show defects in dorsoventral patterning of the neural tube. Although the overall AP patterning of the neural tube is maintained, *HNF-3β* mutant embryos frequently exhibit an absence of expression of the anteriormost markers (Ang and Rossant, 1994; Weinstein et al., 1994). Targeted deletion of another gene expressed in the organizer region, *Lim-1*, profoundly affects formation of the early node and gastrulation movements, and results in formation of embryos lacking head structures. Interestingly, somites and notochord form in *Lim-1* mutant embryos (Shawlot and Behringer, 1995). It is important to note that the zebrafish mutations in this group also vary with respect to the anterior-posterior position of dorsal mesodermal and ectodermal fates they affect. While the *boz*^{m168} mutation affects the entire axial mesoderm (prechordal plate and notochord), *oep*^{m134} and *cyc* mutations affect predominantly prechordal plate, and lead only to mild notochord abnormalities (Yan et al., 1995; Thisse et al., 1994). In contrast, prechordal plate and ventral brain are not affected in the *flh* and *ntl* mutants, despite the absence or reduction of notochord, respectively (Halpern et al., 1993; Talbot et al., 1995). These observations underscore the genetic complexity of the organizer, which reflects its functional complexity (Mangold, 1933). Further analysis of the genes identified in this screen should reveal their relationships with the previously identified genes, and should establish how they interact in the formation and inductive functions of the organizer.

Ventroposterior fates

The second class of mutations in four complementation groups leads to a reduction or malformation of ventral or ventroposterior structures. In addition to tail defects, *ogo*^{m60} and *cpt*^{m52} are characterized by head malformations. It is not clear whether head and tail malformations result from defects in the same genetic pathway(s), or reflect pleiotropic action of these mutations. The ventral and posterior fates are clustered in the ventral marginal region of the zebrafish fate map (Kimmel et al., 1990). During gastrulation this region expresses *eve1* (Joly et al., 1993). In *Xenopus* (Fainsod et al., 1994; Schmidt et al., 1995) and mouse (Jones et al., 1991) this region also expresses BMP-4. The central role of BMP-4 in induction of ventral mesoderm is suggested by several observations. In frogs ectopic expression of BMP-4 inhibits formation of dorsal fates, while a decrease in BMP-4 signaling leads to a reduction of ventroposterior fates (Graff et al., 1994; Schmidt et al., 1995). Moreover, deficiencies in posterior and ventral structures are observed in mouse mutant embryos homozygous for a null mutation in the *BMP-4* gene (Hogan et al., 1994). These phenotypes are similar to phenotypes observed for the *cpt* and *gri* loci. Furthermore, a ventral expansion of the *myoD* expression domain and reduction of ventral markers were observed for the *cpt* and *gri* mutants, similar to *Xenopus* embryos injected with a dominant-negative BMP-4 receptor (Graff et al., 1994; Schmidt et al., 1995). The opposite phenotype of an increased expression domain of *eve1* RNA was demonstrated for *ogo*^{m60} mutant embryos, and in the *kny*^{m119} mutant embryos, *eve1*-expressing cells are localized to ectopic positions. We suggest that genes in this group are likely to regulate specification of ventral fates in the embryo, or to be downstream components of the ventral pathway. Since mutations in *cpt* and *gri* loci lead to reduction of ventral as well as posterior structures in

the embryo, ventral and posterior fates are not only derived from the similar region of the fate map (Kimmel et al., 1990) but also might be dependent on the same genetic pathways.

Perspective

We have identified a group of zygotic effect genes required for pattern formation during zebrafish embryogenesis. Our studies indicate that specification of dorsal and ventroposterior fates, and morphogenetic movements during gastrulation, can be genetically dissected. The identified mutations provide a genetic framework for analysis of inductive and morphogenetic processes during vertebrate embryonic development.

We thank Colleen Boggs, Jane Belak, Laike Stewart, Ioannis Batjakas, Pamela Cohen, Snorri Gunnarson, Jeanine Downing, Heather Goldsboro, Xiaorong Ji and Kristen Diffenbach for invaluable technical help during the various stages of the screen. DNA clones encoding the following genes were kindly provided by our colleagues: *axial* by Uwe Strähle (Strasbourg, France), *eve1* by Jean-Stéphan Joly (Paris, France), *gsc* and *ntl* by Stephan Schulte-Merker (Tübingen, Germany), *pax2* clone by Stephan Krauss (Umea, Sweden). Eric Weinberg (Philadelphia, USA) and Christine and Bernard Thisse (Strasbourg, France) provided us with clones of the *myoD* and *hgg1* genes, respectively, prior to publication. We would like to thank Erez Raz and John Trinkaus for critical reading of the manuscript. This work was supported in part by NIH RO1-HD29761 and a sponsored research agreement with Bristol Myers-Squibb (to W. D.). Further support in the form of fellowships came from HFSP and the Fullbright Program (to Z. R.), EMBO and Swiss National Fund (to A. S.), Helen Hay Whitney Foundation (to D. L. S. and D. Y. S.) and the Damon Runyon-Walter Winchell Cancer Research Fund (to J. M.).

Note added in proof

In collaboration with Dr Mary Mullins, Philadelphia, we have determined that the mutation *m100* (previously named *grinch*) is allelic to *lost-a-fin*, reported by Mullins et al. in this issue. The locus will have the name *lost-a-fin* (*laf*).

REFERENCES

Abdelilah, S., Mountcastle-Shah, E., Harvey, M., Solnica-Krezel, L., Schier, A. F., Stemple, D. L., Malicki, J., Neuhauss, S. C. F., Zwartkruis, F., Stainier, D. Y. R., Rangini, Z. and Driever, W. (1996). Mutations affecting neural survival in the zebrafish, *Danio rerio*. *Development* **123**, 217-227.

Ang, S.-L. and Rossant, J. (1994). HNF-3β is essential for node and notochord formation in mouse development. *Cell* **78**, 561-574.

Beddington, R. S. P. (1994). Induction of a second neural axis by the mouse node. *Development* **120**, 613-620.

Beddington, R. S. P. and Smith, J. C. (1993). Control of vertebrate gastrulation: inducing signal and responding genes. *Cur. Op. Genet. Dev.* **3**, 655-661.

Catala, M., Teillet, M. -A. and Le Douarin, N. (1995). Organization and development of the tail bud analyzed with the quail-chick chimaera system. *Mech. Dev.* **51**, 51-65.

De Robertis, E. M., Fainsod, A., Gont, L. K. and Steinbeisser, H. (1994). The evolution of vertebrate gastrulation. *Development* **1994 Supplement**, 117-124.

Doniach, T., Phillips, C. R., and Gerham, J. C. (1992). Planar induction of anterioposterior pattern in the developing central nervous system of *Xenopus laevis. Science* **257**, 542-544.

Driever, W. (1995). Axis formation in zebrafish. *Curr. Op. Genet. Dev.* **5,** 610-618.

Driever, W., Solnica-Krezel, L., Schier, A. F., Neuhauss, S. C. F., Malicki, J., Stemple, D. L., Stainier, D. Y. R., Zwartkruis, F., Abdelilah, S., Rangini, Z., Belak, J. and Boggs, C. (1996). A genetic screen for mutations affecting embryogenesis in zebrafish. *Development* **123**, 37-46.

Fainsod, A., Steinbeisser, H. and De Robertis, E. M. (1994). On the function of BMP-4 in patterning the marginal zone of the Xenopus embryo. *EMBO J.* **13**, 5015-5025.

Fjose, A., Izpisua-Belmonte, J. C., Fromental-Ramain, C. and Duboule, D. (1994). Expression of the zebrafish gene *hlx-1* in the prechordal plate and during CNS development. *Development* **120**, 71-81.

Gont, L. K., Steinbeisser, H., Blumberg, B. and De Robertis, E. M. (1993). Tail formation as a continuation of gastrulation: the multiple cell populations of the *Xenopus* tail bud derive from the late blastopore lip. *Development* **119**, 991-1004.

Graff, J. M., Thies, R. S., Song, J. J., Celeste, A. J. and Melton, D. A. (1994). Studies with a Xenopus BMP receptor suggest that ventral mesoderm-inducing signals override dorsal signal in vivo. *Cell* **79**, 169-179.

Halpern, M. E., Thisse, C., Ho, R. K., Thisse, B., Riggleman, B., Trevarrow, B., Weinberg, E. S., Postlethwait, J. H. and Kimmel, C. B. (1995). Cell-autonomous shift from axial to paraxial mesoderm development in zebrafish *floating head* mutants. *Development*, **121**, 4257-4264.

Halpern, M. E., Ho, R. K., Walker, C. and Kimmel, C. B. (1993). Induction of muscle pioneers and floor plate is distinguished by the zebrafish *no tail* mutation. *Cell* **75**, 99-111.

Hammerschmidt, M. and Nüsslein-Volhard, C. (1993). The expression of a zebrafish gene homologous to *Drosophila snail* suggests a conserved function in invertebrate and vertebrate gastrulation. *Development* **119**, 1107-1118.

Hatta, K. (1992). Role of the floor plate in axonal patterning in the zebrafish CNS. *Neuron* **9**, 629-642.

Hatta, K., Kimmel, C. B., Ho, R. K. and Walker, C. (1991). The *cyclops* mutation blocks specification of the floor plate of the zebrafish central nervous system. *Nature* **350**, 339-341.

Hatta, K., Püschel, A. W. and Kimmel, C. B. (1994). Midline signaling in the primordium of the zebrafish anterior central nervous system. *Proc. Nat. Acad. Sci. USA* **91**, 2061-2065.

Helde, K. A. and Grunwald, D. J. (1993). The DVR-1 (Vg1) transcript of zebrafish is maternally supplied and distributed throughout the embryo. *Dev. Biol.* **159**, 418-426.

Hemmati-Brivanlou, A., Kelly, O. G. and Melton, D. A. (1994). Follistatin, an antagonist of activin, is expressed in the Spemann organizer and displays direct neuralizing activity. *Cell* **77**, 283-295.

Ho, R. (1992). Axis formation in the embryo of the zebrafish Brachydanio rerio. *Sem. Dev. Biol.* **3**, 53-64.

Ho, R. K. and Kane, D. A. (1990). Cell-autonomous action of zebrafish *spt-1* mutation in specific mesodermal precursors. *Nature* **348**, 728-730.

Hogan, B. L., Blessing, M., Winnier, G. E., Suzuki, N. and Jones, C. M. (1994). Growth factors in development: the role of TGF-β related polypeptide signaling molecules in embryogenesis. *Development* **Supplement**, 53-60.

Holley, S. A., Jackson, P. D., Sasai, Y., Lu, B.,, De Robertis, E. M., Hoffman, F. M. and Ferguson, E. L. (1995). A conserved system for dorsal-ventral patterning in insects and vertebrates involving *sog* and *chordin*. *Nature* **376**, 249-253.

Joly, J. S., Joly, C., Schulte-Merker, S., Boulekbache, H. and Condamine, H. (1993). The ventral and posterior expression of the zebrafish homeobox gene *eve1* is perturbed in dorsalized and mutant embryos. *Development* **119**, 1261-1275.

Jones, C. M., Lyons, K. M. and Hogan, B. L. M. (1991). Involvement of Bone Morphogenetic protein-4 (BMP-4) and Vgr-1 in morphogenesis and neurogenesis in the mouse. *Development* **111**, 531-542.

Kane, D. A. and Warga, R. M. (1994). Domains of movement in the zebrafish gastrula. *Seminars in Dev. Biol.* **5**, 101-109.

Kao, K. R. and Elinson, R. P. (1988). The entire mesodermal mantle behaves as Spemann's organizer in dorsoanterior enhanced Xenopus laevis embryos. *Dev. Biol.* **127**, 64-77.

Keller, R., Clark, W. H., Jr., and Griffin, F. (1991). *Gastrulation. Movements, patterns, and molecules.* New York and London: Plenum Press.

Keller, R. and Danilchik, M. (1988). Regional expression, pattern and timing of convergence and extension during gastrulation of *Xenopus laevis. Development* **103**, 193-209.

Keller, R. and Tibbetts, P. (1989). Mediolateral cell intercalation in the dorsal, axial mesoderm of Xenopus laevis. *Dev. Biol.* **131**, 539-549.

Keller, R. E. (1980). The cellular basis of epiboly: An SEM study of deep cell rearrangements during gastrulation in *Xenopus laevis. J. Embryol. Exp. Morphol.* **60**, 201-234.

Kessler, D. S. and Melton, D. A. (1994). Vertebrate embryonic induction: Mesodermal and neural patterning. *Science* **266**, 596-604.
Kimmel, C. B. (1989). Genetics and early development of zebrafish. *Trends Genet.* **5**, 283-288.
Kimmel, C. B., Ballard, W. W., Kimmel, S. R., Ullmann, B. and Schilling, T. F. (1995). Stages of embryonic development of the zebrafish. *Dev. Dyn.* **203**, 253-310.
Kimmel, C. B., Kane, D. A., Walker, C., Warga, R. M. and Rothman, M. B. (1989). A mutation that changes cell movement and cell fate in the zebrafish embryo. *Nature* **337**, 358-362.
Kimmel, C. B., Warga, R. M. and Schilling, T. F. (1990). Origin and organization of the zebrafish fate map. *Development* **108**, 581-94.
Kintner, C. R. and Melton, D. M. (1987). Expression of *Xenopus N-CAM* RNA is an early response of ectoderm to induction. *Development* **99**, 311-325.
Knapik, E. W., Goodman, A., Atkinson, O. S., Roberts, C. T., Shiozawa, M., Sim, C. U., Weksler-Zangen, S., Trolliet, M. R., Futrell, C., Innes, B. A., Koike, G., McLaughlin, M. G., Pierre, L., Simon, J. S., Vilallonga, E., Roy, M., Chiang, P.-W., Fishman, M. C., Driever, W. and Jacob, H. J. (1996). A reference cross DNA panel for zebrafish (*Danio rerio*) anchored with simple sequence length polymorphisms. *Development* **123**, 451-460.
Krauss, S., Johansen, T., Korzh, V. and Fjose, A. (1991). Expression of the zebrafish paired box gene *pax[zf-b]* during early neurogenesis. *Development* **113**, 1193-206.
Lamb, T. M., Knecht, A. K., Smith, W. C., Stachel, S. E., Economides, A. N., Stahl, N., Yancopolous, G. D. and Harland, R. M. (1993). Neural induction by the secreted polypeptide noggin. *Science* **262**, 713-718.
Mangold, O. (1933). Über die Induktionsfähigkeit der verschiedenen Bezirke der Neurula von Urodelen. *Naturwissenschaften* **21**, 761-766.
Mullins, M. C., Hammerschmidt, M., Haffter, P. and Nüsslein-Volhard, C. (1994). Large-scale mutagenesis in the zebrafish: in search of genes controlling development in a vertebrate. *Curr. Biol.* **4**, 189-202.
Neuhauss, S. C. F., Solnica-Krezel, L., Schier, A. F., Zwartkruis, F., Stemple, D. L., Malicki, J., Abdelilah, S., Stainier, D. Y. R. and Driever, W. (1996). Mutations affecting craniofacial development in zebrafish. *Development* **123**, 357-367.
Nieuwkoop, P. D. (1969). The formation of the mesoderm in urodelean amphibians I. Induction by the endoderm. *Roux's Arch. Dev. Biol.* **162**, 341-373.
Nieuwkoop, P. D. (1992). The formation of the mesoderm in urodelean amphibians. *Roux's Arch. Dev. Biol.* **201**, 18-29.
Oppenheimer, J. (1936). Transplantation experiments on developing teleosts (Fundulus and Perca). *J. Exp. Zool.* **72**, 409-437.
Oxtoby, E. and Jowett, T. (1993). Cloning of the zebrafish *krox-20* gene (*krx-20*) and its expression during hindbrain development. *Nucl. Acids Res.* **21**, 1087-1095.
Püschel, A. W., Westerfield, M. and Dressler, G. R. (1992). Comparative analysis of Pax-2 protein distributions during neurulation in mice and zebrafish. *Mech. Dev.* **38**, 197-208.
Sasai, Y., Lu, B., Steinbeisser, H., Geissert, Gont, L. and De Robertis, E. M. (1994). Xenopus chordin: a novel dorsalizing factor activated by organizer-specific homeobox genes. *Cell* **79**, 779-790.
Sater, A. K., Steinhardt, R. A. and Keller, R. (1993). Induction of neuronal differentiation by planar signals in Xenopus embryos. *Dev. Dyn.* **197**, 268-280.
Scharf, S. R. and Gerhart, J. C. (1983). Axis determination in eggs of Xenopus laevis*:* A critical period before first cleavage, identified by the common effects of cold, pressure and ultraviolet irradiation. *Dev. Biol.* **99**, 75-87.
Schier, A. F., Neuhauss, S. C. F., Harvey, M., Malicki, J., Solnica-Krezel, L., Stainier, D. Y. R., Zwartkruis, F., Abdelilah, S., Stemple, D. L., Rangini, Z., Yang, H. and Driever, W. (1996). Mutations affecting the development of the embryonic zebrafish brain. *Development* **123**, 165-178.
Schmidt, J. E., Suzuki, A., Ueno, N. and Kimelman, D. (1995). Localized BMP-4 mediates dorsal/ventral patterning in the early Xenopus embryo. *Dev. Biol.* **169**, 37-50.
Schoenwolf, G. C. (1991). Cell movements in the epiblast during gastrulation and neurulation in avian embryos. *In Gastrulation. Movements, patterns, and molecules.* (ed. R. Keller). New York and London: Plenum Press.
Schulte-Merker, S., Hammerschmidt, M., Beuchle, D., Cho, K. W., De Robertis, E. M. and Nüsslein-Volhard, C. (1994). Expression of zebrafish *goosecoid* and *no tail* gene products in wild-type and mutant *no tail* embryos. *Development* **120**, 843-852.
Schulte-Merker, S., Ho, R. K., Herrmann, B. G. and Nüsslein-Volhard, C. (1992). The protein product of the zebrafish homologue of the mouse *T* gene is expressed in nuclei of the germ ring and the notochord of the early embryo. *Development* **116**, 1021-1032.
Schulte-Merker, S., VanEeden, F. J. M., Halpern, M. E., Kimmel, C. B. and Nüsslein-Volhard, C. (1994). *No tail* (*Ntl*) is the zebrafish homologue of the mouse *T* (*Brachyury*) gene. *Development* **120**, 1009-1015.
Shawlot, W., and Behringer, R. R. (1995). Requirement for *Lim1* in head-organizer function. *Nature* **374**, 425-430.
Shih, J. and Keller, R. (1992). Cell motility driving mediolateral intercalation in explants of *Xenopus laevis*. *Development* **116**, 901-914.
Sive, H. L. (1993). The frog prince-ss: A molecular formula for dosoventral patterning in Xenopus. *Genes Dev.* **7**, 1-12.
Slack, J. M. (1994). Inducing factors in Xenopus early embryos. *Curr. Biol.* **4**, 116-126.
Smith, W. C. and Harland, R. M. (1991). Injected *Xwnt-8* RNA acts early in Xenopus embryos to promote formation of a vegetal dorsalizing center. *Cell* **67**, 753-765.
Sokol, S., Christian, J. L., Moon, R. T. and Melton, D. A. (1991). Injected *Wnt* RNA induces a complete body axis in Xenopus embryos. *Cell* **67**, 741-752.
Solnica-Krezel, L. and Driever, W. (1994). Microtubule arrays of the zebrafish yolk cell: organization and function during epiboly. *Development* **120**, 2443-2455.
Solnica-Krezel, L., Schier, A. F. and Driever, W. (1994). Efficient recovery of ENU-induced mutations from the zebrafish germline. *Genetics* **136**, 1401-1420.
Solnica-Krezel, L., Stemple, D. L. and Driever, W. (1995). Transparent things: Cell fates and cell movements during early embryogenesis of zebrafish. *BioEssays*, **17**, 931-939.
Spemann, H. (1938). *Embryonic Development and Induction.* New Haven, CT: Yale University Press.
Stachel, S. E., Grunwald, D. J. and Myers, P. Z. (1993). Lithium perturbation and *goosecoid* expression identify a dorsal specification pathway in the pregastrula zebrafish. *Development* **117**, 1261-1274.
Stemple, D. L., Solnica-Krezel, L., Zwartkruis, F., Neuhauss, S. C. F., Schier, A. F., Malicki, J., Stainier, D. Y. R., Abdelilah, S., Rangini, Z., Mountcastle-Shah, E. and Driever, W. (1996). Mutations affecting development of the notochord in zebrafish. *Development* **123**, 117-128.
Strähle, U., Blader, P., Henrique, D. and Ingham, P. W. (1993). *Axial*, a zebrafish gene expressed along the developing body axis, shows altered expression in *cyclops* mutant embryos. *Genes Dev.* **7**, 1436-1446.
Streisinger, G., Walker, C., Dower, N., Knauber, D. and Singer, F. (1981). Production of clones of homozygous diploid zebrafish (Brachydanio rerio). *Nature* **291**, 293-296.
Talbot, W. S., Trevarrow, B., Halpern, M. E., Melby, A. E., Farr, G., Postlethwait, J. H., Jowett, T., Kimmel, C. B. and Kimelman, D. (1995). A homeobox gene essential for zebrafish notochord development. *Nature* **378**, 150-157.
Thisse, C., Thisse, B., Halpern, M. E. and Postlethwait, J. H. (1994). *Goosecoid* expression in neurectoderm and mesendoderm is disrupted in zebrafish cyclops gastrulas. *Dev. Biol.* **164**, 420-429.
Thisse, C., Thisse, B., Schilling, T. F. and Postlethwait, J. H. (1993). Structure of the zebrafish *snail1* gene and its expression in wild-type, *spadetail* and *no tail* mutant embryos. *Development* **119**, 1203-1215.
Thomsen, G., Woolf, T., Whitman, M., Sokol, S., Vaughan, J., Vale, W. and Melton, D. A. (1990). Activins are expressed early in Xenopus embryogenesis and can induce axial mesoderm and anterior structures. *Cell* **63**, 485-493.
Thomsen, G. H. and Melton, D. A. (1993). Processed Vg1 protein is an axial mesoderm inducer in Xenopus. *Cell* **74**, 433-441.
Trinkaus, J. P. (1951). A study of the mechanism of epiboly in the egg of Fundulus heteroclitus. *J. Exp. Zool.* **118**, 269-320.
Trinkaus, J. P. (1984a) *Cells into Organs. The forces that Shape the Embryo.* London: Prentice Hall International.
Trinkaus, J. P. (1984b). Mechanism of *Fundulus* epiboly - A current view. *Amer. Zool.* **24**, 673-688.
Trinkaus, J. P., Trinkaus, M., and Fink, R. (1992). On the convergent cell movements of gastrulation in Fundulus. *J. Exp. Zool.* **261**, 40-61.
Tucker, A. S., and Slack, J. M. W. (1995). The Xenopus tail forming region. *Development* **121**, 249-262.
Waddington, C. H. (1933). Induction by the primitive streak and its derivatives in the chick. *J. Exp. Biol.* **10**, 38-46.
Warga, R. M. and Kimmel, C. B. (1990). Cell movements during epiboly and gastrulation in zebrafish. *Development* **108**, 569-80.

Weinberg, E. S., Allende, M. L., Kelly, C. S., Murakami, T., Abdelhamid, A., Andermann, P., Doerre, G., Grunwald, D. J., and Riggleman, B. (1996). Developmental regulation of Zebrafish *MyoD* in wild-type, *no tail*, and *spadetail* embryos. *Development* **122,** 271-280.

Weinstein, D. C., Ruiz i Altaba, A., Chen, W. S., Hoodless, P., Prezioso, V. R., Jessel, T. M., and Darnell, J. E., Jr. (1994). The winged-helix transcription factor *HNF-3β* is required for notochord development in the mouse embryo. *Cell* **78**, 575-588.

Westerfield, M. (1994). *The Zebrafish Book*. Eugene: University of Oregon Press.

Wilson, E. T., Cretekos, C. J. and Helde, K. A. (1995). Cell mixing during early epiboly in the zebrafish embryo. *Dev. Genet.* **17**, 6-15.

Wilson, P. and Keller, R. (1991) Cell rearrangement during gastrulation of *Xenopus*: direct observation of cultured explants. *Development,* **112**, 289-300.

Yan, Y.-L., Hatta, K., Riggleman, B. and Postlethwait, J. H. (1995). Expression of a type II collagen gene in the zebrafish embryonic axis. *Dev. Dyn.* **203**, 363-376.

Zekeri, Z. F., Quaglino, D., Latham, T., and Lockshin, R. A. (1993). Delayed internucleosomal DNA fragmentation in programmed cell death. *FASEB J.* **7**, 470-478.

(Accepted 8 January 1996)